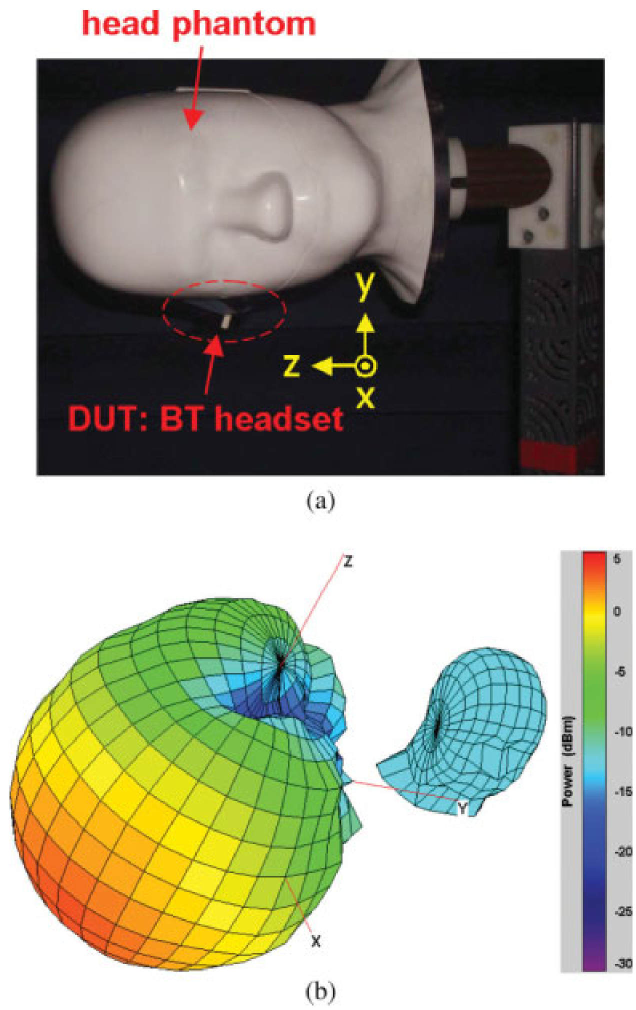

Figure 6 Measured peak EIRP for the design integrated in a functioning Bluetooth headset attached to a head phantom: (a) test setup; (b) 3D EIRP patterns in Channel 39. [Color figure can be viewed in the online issue, which is available at www.interscience.wiley.com]

a compact wireless device where the system circuit board is small and short, and the layout therein does not tolerate further extra matching circuit.

REFERENCES

1. L. Lu and J.C. Coetzee, Reduced-size microstrip patch antenna for Bluetooth applications, Electron Lett 41 (2005), 944–945.
2. K.L. Wong, M.R. Hsu, W.Y. Li, and S.W. Su, Study of the Bluetooth headset antenna with the user's head, Microwave Opt Technol Lett 49 (2007), 19–23.
3. C.H. Wu, K.L. Wu, Y.C. Lin, and S.W. Su, Internal shorted monopole antenna for the watch-type wireless communication device for Bluetooth operation, Microwave Opt Technol Lett 49 (2007), 942–946.
4. D.H. Seo, S.G. Jeon, N.K. Kang, J.I. Ryu, and J.H. Choi, Design of a novel compact antenna for a Bluetooth LTCC module, Microwave Opt Technol Lett 50 (2008), 180–183.
5. J.H. Yoon, Design of a compact antenna for Bluetooth application, Microwave Opt Technol Lett 50 (2008), 2568–2572.
6. T.Y. Wu and K.L. Wong, On the impedance bandwidth of a planar inverted-F antenna for mobile handsets, Microwave Opt Technol Lett 32 (2002), 249–251.
7. M.C. Huynh and W. Stutzman, Ground plane effects on planar inverted-F antenna (PIFA) performance, IEE Proc Microwave Antennas Propag 150 (2003), 209–213.
8. S.W. Su, C.H. Wu, W.S. Chen, and K.L. Wong, Broadband printed π-shaped monopole antenna for WLAN operation, Microwave Opt Technol Lett 41 (2004), 269–279.
9. K.L. Wong, J.H. Chou, and S.W. Su, Isolation between GSM/DCS and WLAN antennas in a PDA phone, Microwave Opt Technol Lett 45 (2005), 347–352.
10. CTIA Authorized Test Laboratory, CTIA, The wireless association. Available at: http://www.ctia.org/business_resources/certification/test_labs/.

SIMPLE SMALL-SIZE COUPLED-FED UNIPLANAR PIFA FOR MULTIBAND CLAMSHELL MOBILE PHONE APPLICATION

Ting-Wei Kang and Kin-Lu Wong
Department of Electrical Engineering, National Sun Yat-Sen University, Kaohsiung 80424, Taiwan; Corresponding author: kangtw@ema.ee.nsysu.edu.tw

Received 6 March 2009

ABSTRACT: *In this study, a simple uniplanar printed PIFA occupying a small area of 10 × 40 mm² for achieving multiband operation in the clamshell mobile phone is presented. The proposed PIFA is formed by a simple shorted radiating strip coupled-fed by a simple feeding strip and is mounted at the hinge of the clamshell mobile phone; further, the upper ground plane is connected to the main ground plane using an extended connecting strip. With the coupling feed and the connection arrangement between the main and upper ground planes, the proposed PIFA itself is not only an efficient radiator, it can also excite the two ground planes of the clamshell mobile phone as an efficient radiator (dipole-like resonant modes are excited). Thus, with a small occupying area and a simple structure for the proposed PIFA, two wide operating bands at lower and higher frequencies can be provided to cover GSM850/900/1800/1900/UMTS bands for WWAN operation. The antenna also meets the 1-g SAR specification of 1.6 W/kg required for practical applications.* © 2009 Wiley Periodicals, Inc. Microwave Opt Technol Lett 51: 2805–2810, 2009; Published online in Wiley InterScience (www.interscience.wiley.com). DOI 10.1002/mop.24756

Key words: *antennas; mobile antennas; handset antennas; PIFA; multiband antennas*

1. INTRODUCTION

Because of the rapid development in the mobile communication systems, multiband operation, especially the pentaband operation of GSM850/900/1800/1900/UMTS, for wireless wide area network (WWAN) communications has been demanded for many modern mobile phones. To meet the multiband operation requirement, the conventional planar inverted-F antennas (PIFAs), such as in [1–6], that are promising to be applied in the mobile phone as the internal antennas often require the use of at least two resonant strips or patches for obtaining more resonant modes to cover the desired multiband operation. As a result, the occupied volume of the multiband PIFAs is usually increased as additional resonant strips or patches are added. The increasing volume makes such conventional multiband PIFAs less attractive for practical applications in the modern mobile phones.

In this article, we present a small-size PIFA capable of generating two wide operating bands at lower and higher frequencies to cover GSM850/900 (824–894/880–960 MHz) and

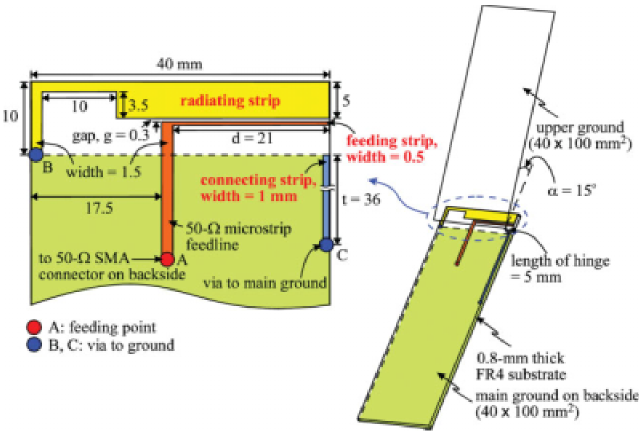

Figure 1 Geometry of the proposed coupled-fed PIFA for a clamshell mobile phone in the open state (talk condition). [Color figure can be viewed in the online issue, which is available at www.interscience.wiley.com]

GSM1800/1900/UMTS (1710–1880/1850–1990/1920–2170 MHz) operations in the clamshell mobile phone. Note that the clamshell or folder-type mobile phone [7–15] is attractive for mobile users because of its capability of accommodating a large display for multimedia communications. The proposed PIFA has a simple uniplanar structure formed by a single radiating strip coupled-fed by a feeding strip and is easily printed on a small area of 10 × 40 mm^2 only. By applying the proposed PIFA at the hinge of the clamshell mobile phone, whose two ground planes (the upper and main ground planes) are connected through an extended connecting strip of proper length, both the PIFA and the two ground planes can be efficient radiators. Efficient dipole-like resonant modes (0.5λ and 1.0λ modes) can be excited and fine-adjusted to be at about 900 and 1700 MHz for covering GSM850/900/1800 operations. Also note that the excited 0.5λ dipole-like resonant mode at about 900 MHz has a dual-resonant behavior caused by the use of the coupling feed, hence resulting in a wide operating band capable of covering GSM850/900 operations.

With the excited dipole-like resonant modes contributed by the two ground planes of the clamshell mobile phone, the proposed PIFA is only required to provide a resonant mode for covering GSM1900 and UMTS bands. For this reason, only one short resonant strip for the proposed PIFA is required, which is about 50 mm only, in this study. This behavior leads to a small printed area of 10 × 40 mm^2 required for the proposed PIFA. In addition to the small size, the proposed PIFA is easy to fabricate, because of its much less complicated structure when compared with those of the conventional multiband PIFAs [1–6]. Moreover, when the clamshell mobile phone is in the idle condition where the upper ground plane is parallel to the main ground plane (the closed state), different from the talk condition (α = 15° in Fig. 1, the open state), the proposed PIFA is still promising to cover WWAN operation over the five operating bands with acceptable radiation efficiency. The specific absorption rate (SAR) [16–18] results in 1 g of head tissue from exposure to the antenna radiation of the studied clamshell mobile phone are also tested. The obtained SAR results meet the specification of 1.6 W/kg required for practical applications. Details of the proposed antenna and obtained results are presented and discussed.

2. PROPOSED COUPLED-FED PIFA

Figure 1 shows the geometry of the proposed coupled-fed PIFA for a clamshell mobile phone in the open state (talk condition). In this case, the upper ground plane as the cover of the clamshell mobile phone has an angle of $\alpha = 15°$ to the main ground plane of the clamshell mobile phone. In this study, the upper ground plane is fabricated using a 0.2-mm-thick copper plate; the main ground plane is printed on a 0.8-mm-thick FR4 substrate treated as the main circuit board of the clamshell mobile phone studied here. The two ground planes have the same dimensions of 40 × 100 mm^2 and are connected through a 1-mm wide extended connecting strip of length 5 mm at the hinge and 36 mm (t) printed on the main circuit board. Through point C in the main circuit board, the connecting strip connects the upper ground plane to the main ground plane. By selecting a proper length t (36 mm here) of the connecting strip, the 0.5λ and 1.0λ dipole-like resonant modes contributed by the two ground planes at about 900 and 1700 MHz can be excited. Detailed results of the connecting strip are analyzed in Section 3 with the aid of Figure 3.

The proposed PIFA is printed on the small area of 10 × 40 mm^2 on the top portion of the main circuit board and is at the hinge of the clamshell mobile phone. The PIFA is formed by a simple inverted-L radiating strip coupled-fed by a simple feeding strip. The radiating strip is short-circuited to the top edge of the main ground plane through point B and provides a resonant path of about 50 mm. Through a small coupling gap of 0.3 mm (g), the radiating strip is capacitively excited by the feeding strip of length 21 mm (d) and width 0.5 mm, which is connected to the 50-Ω microstrip feedline of width 1.5 mm printed on the front surface of the main circuit board for testing the antenna in this study. Because of the use of the coupling feed, the large inductive reactance of the input impedance observed for frequencies at around 900 MHz is compensated. Furthermore, the large resistance of the input impedance at around 900 MHz can also be decreased to be close to 50 Ω. This behavior is similar to the coupled-fed PIFA applied to the bar-type mobile phone studied in [19, 20] and leads to the dual-resonant excitation of the 0.5λ dipole-like resonant mode in this study. Hence, a wide operating band of about 300 MHz for the antenna's lower band to cover GSM850/900 operations is obtained in this study. Detailed results are presented in Figures 4 and 5 and will be discussed in the next section.

The proposed PIFA also generates a wide operating band at about 2.3 GHz for covering GSM1900/UMTS operations. The open-end section of the radiating strip is widened for achieving bandwidth enhancement in the excited resonant mode, which has been known to be an effective design in improving the bandwidth [6, 21]. The resonant mode contributed by the PIFA itself also shows a dual-resonant behavior and hence provides a wide operating band for the desired GSM1900/UMTS operations. This resonant mode incorporating the 1.0λ dipole-like resonant mode contributed by the two ground planes forms a very wide operating band of larger than 1 GHz for the antenna's upper band to cover GSM1800/1900/UMTS operations.

3. RESULTS AND DISCUSSION

The proposed antenna was fabricated and tested. Figure 2 shows the measured and simulated return loss for the fabricated prototype in the open state. Good agreement between the measured data and the simulated results obtained using Ansoft HFSS [22] is observed. From these results, two wide operating bands are obtained. The lower operating band is formed by a dual-resonant mode and has a large 3:1 VSWR bandwidth of 290 MHz (750–1040 MHz), allowing the antenna to easily cover GSM850/900 operations. A very large bandwidth of about 1.2 GHz (1580–

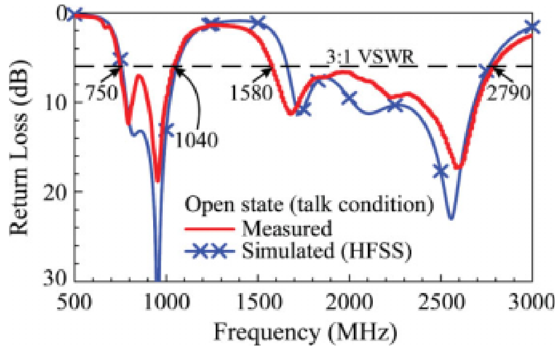

Figure 2 Measured and simulated return loss for the proposed antenna in the open state ($\alpha = 15°$). [Color figure can be viewed in the online issue, which is available at www.interscience.wiley.com]

2790 MHz) is also obtained for the upper operating band to cover GSM1800/1900/UMTS operations. Note that the bandwidth definition of 3:1 VSWR (6-dB return loss) is generally used for internal WWAN mobile phone antennas in practical applications.

To analyze the effects of the coupling feed and the connecting strip in the proposed antenna, the simulated return loss for the reference antenna (corresponding PIFA with a direct feed shown in the figure) as a function of the connecting-strip length t is first studied. All the dimensions are the same as given in Figure 1, except that the reference antenna uses a direct feed. Results for the length $t = 0$, 31, 36, and 41 mm are presented in Figure 3(a). Except for the case of $t = 0$, there are three resonant modes excited (Modes 1, 2, and 3 shown in the figure). It is observed that the variations in the length t show very small effect on the Mode 3; this behavior is reasonable, since the Mode 3 is mainly contributed by the PIFA itself, not the two ground planes of the clamshell mobile phone. For the Mode 2, it cannot be excited for the case of $t = 0$. With the proper length t selected, the Mode 2 can be excited (see the cases of $t = 31$, 36, and 41 mm). This is largely because the connecting strip can perturb the surface current distributions excited on the two ground planes such that the null or very small currents no longer exist at around the hinge position or in-between the two ground planes [see the excited surface current distribution at 1700 MHz shown in Fig. 3(b)]; in this case, the 1.0λ dipole-like resonant mode is promising to be excited. This behavior is similar to that used for achieving a wideband monopole antenna for DTV/GSM operation in the mobile phone in [23]. Further, a longer connecting strip can increase the effective resonant length of the 1.0λ dipole-like mode, which makes the Mode 2 shifted to lower frequencies with increasing length t as shown in the figure. This shifting in frequency is also observed in Figure 3(a) for the Mode 1 (the 0.5λ dipole-like mode), whose excited surface current distribution for the case of $t = 36$ mm is shown in Figure 3(b).

By further application of the coupling feed to the reference antenna (that is, the proposed antenna in Fig. 1), dual-resonant excitation for the Mode 1 at about 900 MHz can be excited to achieve a wide operating band covering GSM850/900 operations. To demonstrate this result, Figure 4 presents the simulated return loss and input impedance for the proposed antenna studied in Figure 2 and the reference antenna with $t = 36$ mm studied in Figure 3. From these results, small effects on the Modes 2 and 3 are seen. For the Mode 1, the coupling feed effectively decreases the large input resistance and reactance, which is similar to those observed in [18, 19]. Small variations in the input resistance and reactance for frequencies at around the Mode 1 are also seen [see Fig. 4(b)]. These results lead to good dual-resonant excitation for the Mode 1, and enhanced bandwidth is hence obtained.

Detailed effects of the parameters of the coupling feed are studied in Figures 5 and 6. The simulated return loss for the proposed antenna as a function of the coupling-gap width g is presented in Figure 5, in which the results for the width g varied from 0.2 to 0.6 mm are shown. Large effects on the Mode 1 are seen, whereas relatively very small effects on the Modes 2 and 3 are observed. Figure 6 shows the simulated return loss for the proposed antenna as a function of the coupling-strip length d, and results of the length d varied from 17 to 21 mm are presented. Similar behavior as in Figure 6 is seen. The results indicate that by adjusting the width g and the length d in the coupling feed, the coupling effects can be effectively controlled and good dual-resonant excitation of the Mode 1 can be obtained.

Figure 7 shows the measured three-dimensional (3D) radiation patterns at 859, 925, 1795, 1920, and 2045 MHz (central

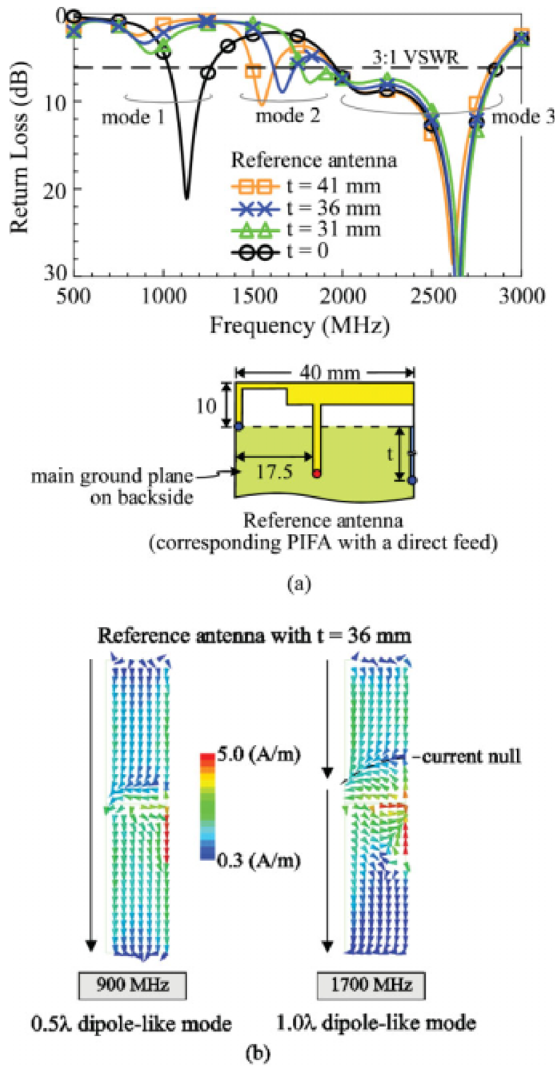

Figure 3 (a) Simulated return loss for the reference antenna (corresponding PIFA with a direct feed) as a function of the connecting-strip length t. (b) Simulated surface current distributions at 900 and 1700 MHz for the reference antenna with $t = 36$ mm. [Color figure can be viewed in the online issue, which is available at www.interscience.wiley.com]

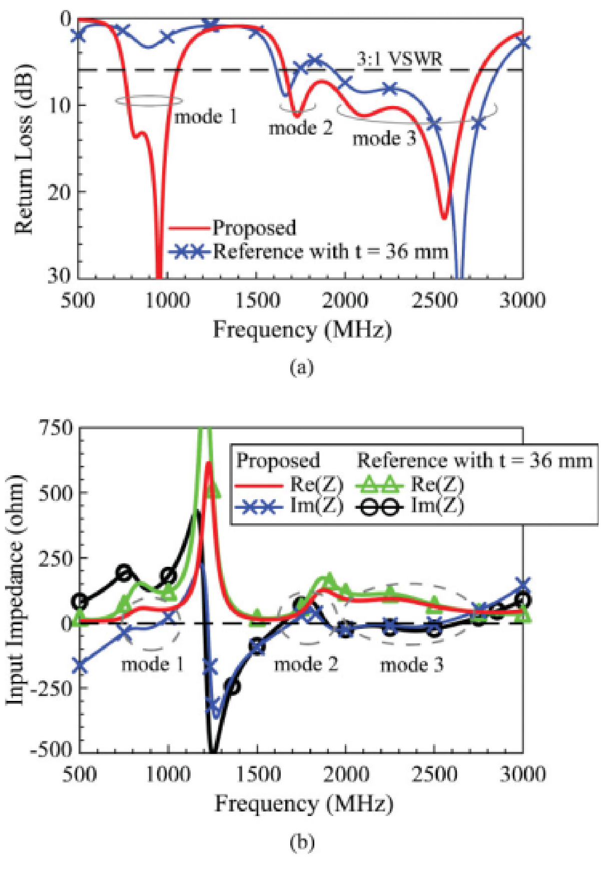

Figure 4 Simulated (a) return loss and (b) input impedance for the proposed antenna studied in Figure 2, and the reference antenna with $t = 36$ mm studied in Figure 3. [Color figure can be viewed in the online issue, which is available at www.interscience.wiley.com]

frequencies of the five operating bands) for the proposed antenna studied in Figure 2. Dipole-like radiation patterns at 859, 925, and 1795 MHz are seen, which are operating frequencies over the Modes 1 and 2 (0.5λ and 1.0λ dipole-like resonant modes) as discussed in Figures 3 and 4. For 1920 and 2045 MHz (operating frequencies over the Mode 3), more variations in the obtained radiation patterns are seen and are different from that for 1795 MHz. This is reasonable, since the operating characteristics of the Mode 3 are different from that of the Mode 2.

The measured radiation efficiency and antenna gain for the proposed antenna are studied in Figure 8. Over the GSM850/

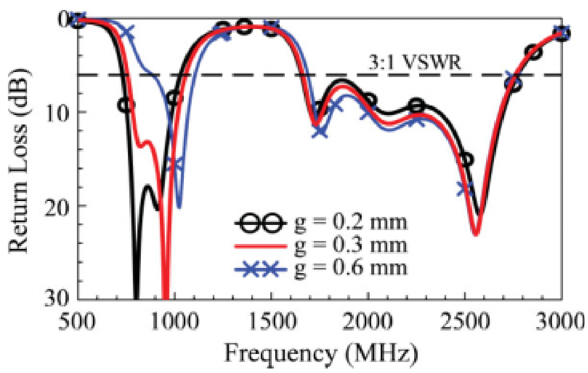

Figure 5 Simulated return loss for the proposed antenna as a function of the coupling-gap width *g*. [Color figure can be viewed in the online issue, which is available at www.interscience.wiley.com]

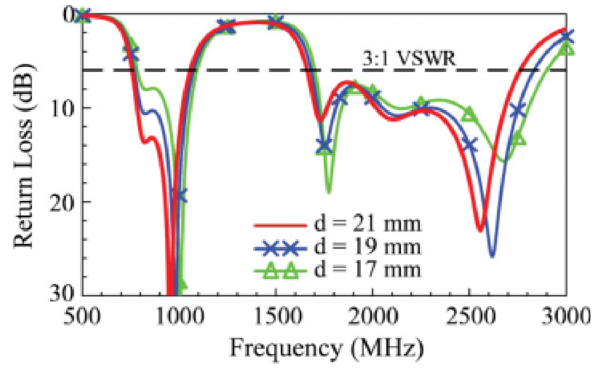

Figure 6 Simulated return loss for the proposed antenna as a function of the coupling-strip length *d*. [Color figure can be viewed in the online issue, which is available at www.interscience.wiley.com]

900 bands shown in Figure 8(a), the radiation efficiency is varied in a small range of about 77–89%. Small variations of less than 1 dB in the antenna gain (about 1.6–2.5 dBi) are also observed. For the GSM1800/1900/UMTS bands shown in Figure 8(b), the radiation efficiency ranges from about 60–92%, and the antenna gain is varied from about 2.0–3.6 dBi. The obtained radiation characteristics are good for practical applications.

For the clamshell mobile phone, it is noted that the ground-plane condition varies greatly when it is in the open state (talk condition) and the closed state (idle condition). Hence, the antenna performances for the clamshell mobile phone in the closed state should be studied. Figure 9 shows the comparison of the measured return loss for the proposed antenna in the open state ($\alpha = 15°$) and the closed state ($\alpha = 180°$). Over the five operating bands, the measured return loss is generally better than 6:1 VSWR (3-dB return loss), which is acceptable for internal WWAN antennas in the idle condition of the clamshell mobile phone applications. Figure 10 also shows the comparison of the measured radiation efficiency for the proposed antenna in the open state ($\alpha = 15°$) and the close state ($\alpha = 180°$). Over the GSM850/900 bands in Figure 10(a), the radiation efficiency in the closed state is varied from about 33–56%, decreased by about 1.4–3.5 dB when compared with that in the open state. For the GSM1800/1900/UMTS bands in Figure 10(b), the radiation efficiency in the closed state ranges from about 30–54% and is lowered by about 1.0–3.3 dB than that in the open state. The obtained results indicate that the proposed antenna is

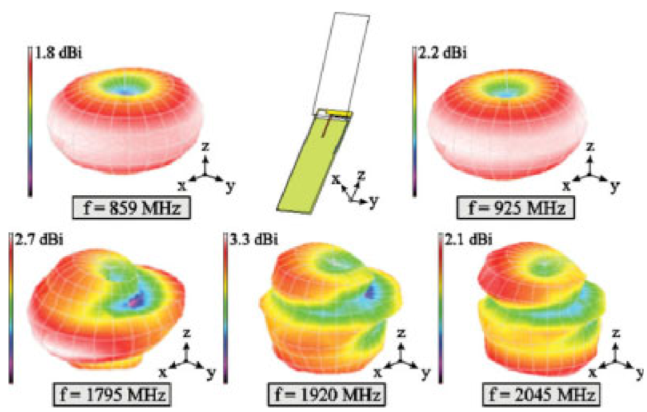

Figure 7 Measured 3D radiation patterns for the proposed antenna studied in Figure 2. [Color figure can be viewed in the online issue, which is available at www.interscience.wiley.com]

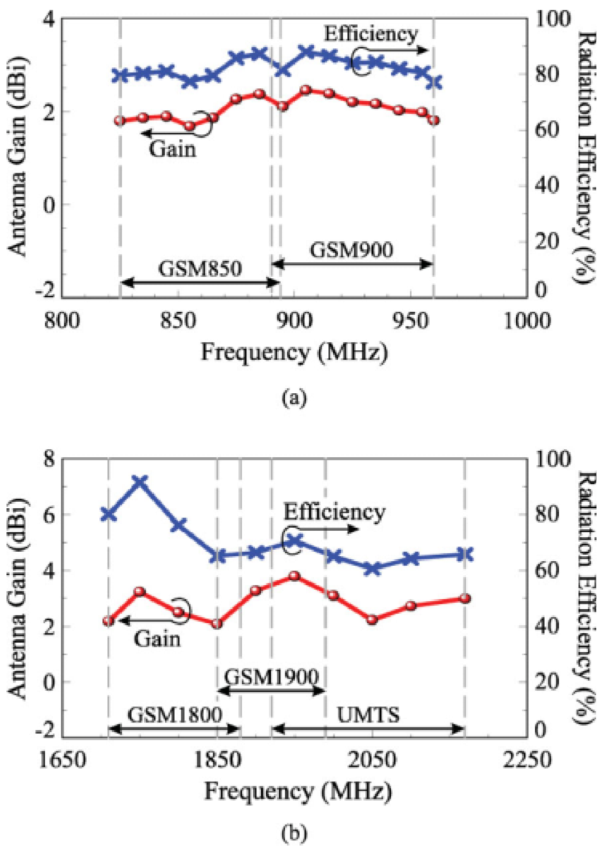

Figure 8 Measured radiation efficiency and antenna gain for the proposed antenna studied in Figure 2. (a) The GSM850/900 bands and (b) the GSM1800/1900/UMTS bands. [Color figure can be viewed in the online issue, which is available at www.interscience.wiley.com]

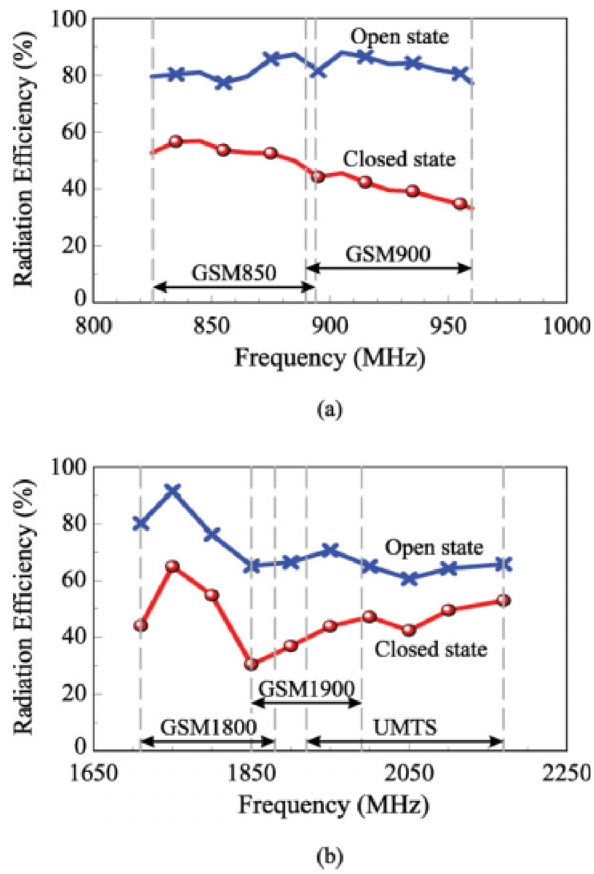

Figure 10 Comparison of the measured radiation efficiency for the proposed antenna in the open state ($\alpha = 15°$) and the close state ($\alpha = 180°$). (a) The GSM850/900 bands and (b) the GSM1800/1900/UMTS bands. [Color figure can be viewed in the online issue, which is available at www.interscience.wiley.com]

promising for the clamshell mobile phone application in both the open and closed states.

The SAR results of the proposed antenna were also studied. Figure 11 shows the SAR simulation model provided by SEMCAD [24]. The upper ground plane is spaced 5 mm to the phantom head for considering the housing of the clamshell mobile phone. The obtained SAR results in 1 g of head tissue from exposure to the antenna radiation are listed in Table 1. At 859 and 925 MHz, the SAR is tested using 24 dBm (2-W continuous input power with a user channel being 1/8 of a time slot), whereas at 1795, 1920, and 2045 MHz, the SAR is tested using 21 dBm (1-W continuous input power with a user channel being 1/8 of a time slot at 1795 and 1920 MHz and 0.125-W continuous input power at 2045 MHz). The obtained SAR results are all much smaller than the 1-g SAR specification of 1.6 W/kg required for practical applications.

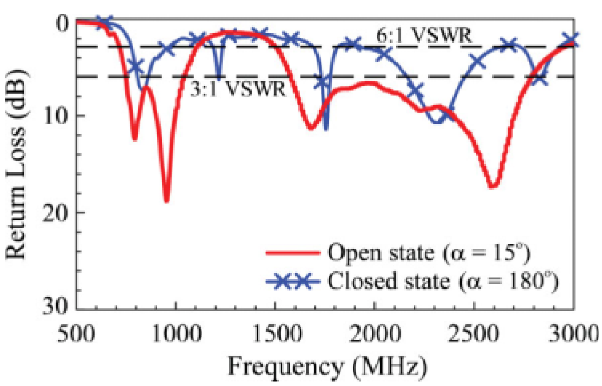

Figure 9 Comparison of the measured return loss for the proposed antenna in the open state ($\alpha = 15°$) and the closed state ($\alpha = 180°$). [Color figure can be viewed in the online issue, which is available at www.interscience.wiley.com]

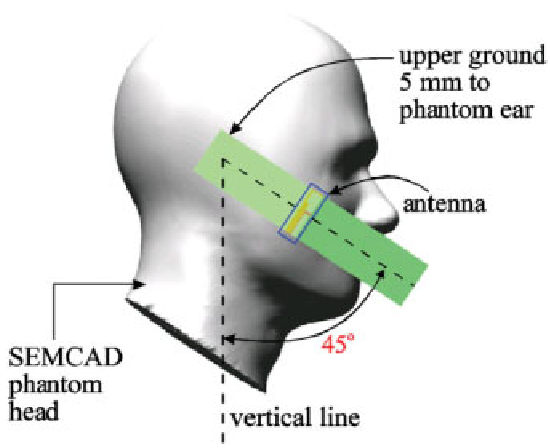

Figure 11 SAR simulation model (SEMCAD [24]) for the proposed antenna with the user's head. [Color figure can be viewed in the online issue, which is available at www.interscience.wiley.com]

TABLE 1 Simulated SAR in 1-g Head Tissue Obtained from SEMCAD [24] for the SAR Simulation Model in Figure 11

	Simulated SAR				
Frequency (MHz)	859	925	1795	1920	2045
1-g SAR (W/kg)	0.70	0.72	0.53	0.56	0.50

4. CONCLUSIONS

In this study, a uniplanar printed PIFA with simple configuration and small size (10×40 mm^2) for pentaband WWAN operation in the clamshell mobile phone has been proposed and studied. The proposed antenna successfully uses the two ground planes of the clamshell mobile phone as an efficient radiator for covering the lower frequencies of the desired pentaband operation, while the printed PIFA itself is for generating a resonant mode for covering only the higher frequencies. This leads to a small printed area required for the proposed antenna. Good radiation characteristics over the five operating bands have also been obtained for the proposed antenna applied in the clamshell mobile phone in the open state (talk condition) and the closed state (idle condition) as well. The obtained SAR results in 1-g head tissue from exposure to the radiation of the proposed antenna are found to be less than 0.8 W/kg, much less than the SAR limit of 1.6 W/kg required for practical applications.

REFERENCES

1. K.L. Wong, Planar antennas for wireless communications, Wiley, New York, 2003.
2. Y.X. Guo, M.Y.W. Chia, and Z.N. Chen, Miniature built-in multiband antennas for mobile handsets, IEEE Trans Antennas Propag 52 (2004), 1936–1944.
3. Y.S. Shin, B.N. Kim, W.I. Kwak, and S.O. Park, GSM/DCS/IMT-2000 triple-band built-in antenna for wireless terminals, IEEE Antennas Wireless Propag Lett 3 (2004), 104–107.
4. M.Z. Azad and M. Ali, A miniaturized Hilbert PIFA for dual-band mobile wireless applications, IEEE Antennas Wireless Propag Lett 4 (2005), 59–62.
5. K.L. Wong, Y.C. Lin, and T.C. Tseng, Thin internal GSM/DCS patch antenna for a portable mobile terminal, IEEE Trans Antennas Propag 54 (2006), 238–242.
6. K.L. Wong, Y.C. Lin, and B. Chen, Internal patch antenna with a thin air-layer substrate for GSM/DCS operation in a PDA phone, IEEE Trans Antennas Propag 55 (2007), 1165–1172.
7. M. Tzortzakakis and R.J. Langley, Quad-band internal mobile phone antenna, IEEE Trans Antennas Propag 55 (2007), 2097–2103.
8. B.S. Collins, Improving the RF performance of clamshell handsets, In: Proc IEEE International Workshop on Antenna Technology: Small Antennas and Metamaterials, 2006, IEEE, 265–268.
9. K.L. Wong, S.W. Su, C.L. Tang, and S.H. Yeh, Internal shorted patch antenna for a UMTS folder-type mobile phone, IEEE Trans Antennas Propag 53 (2005), 3391–3394.
10. P.L. Teng, T.W. Chiou, and K.L. Wong, Internal planar monopole antenna for GSM/DCS/PCS folder-type mobile phone, Microwave Opt Technol Lett 39 (2003), 106–108.
11. T. Sugiyama, H. Horita, Y. Shirakawa, M. Ikegaya, S. Takaba, and H. Tate, Triple-band internal antenna for clamshell type mobile phone, Hitachi Cable Rev (2003), 26–31.
12. P.L. Teng, T.W. Chiou, and K.L. Wong, Planar inverted-F antenna with a bent, meandered radiating arm for GSM/DCS operation, Microwave Opt Technol Lett 38 (2003), 73–75.
13. C.I. Lin and K.L. Wong, Printed monopole slot antenna for penta-band operation in the folder-type mobile phone, Microwave Opt Technol Lett 50 (2008), 2237–2241.
14. K.L. Wong and S.Y. Tu, Ultra-wideband coupled-fed loop antenna for penta-band folder-type mobile phone, Microwave Opt Technol Lett 50 (2008), 2706–2712.
15. C.H. Chang, K.L. Wong, and J.S. Row, Coupled-fed small-size PIFA for penta-band folder-type mobile phone application, Microwave Opt Technol Lett 51 (2009), 18–23.
16. J.C. Lin, Specific absorption rates induced in head tissues by microwave radiation from cell phones, Microwave 2 (2001), 22–25.
17. O. Kivekas, J. Ollikainen, T. Lehtiniemi, and P. Vainikainen, Bandwidth, SAR, and efficiency of internal mobile phone antennas, IEEE Trans Electromagn Compat 46 (2004), 71–86.
18. Y.W. Chi and K.L. Wong, Compact multiband folded loop chip antenna for small-size mobile phone, IEEE Trans Antennas Propag 56 (2008), 3797–3803.
19. K.L. Wong and C.H. Huang, Bandwidth-enhanced internal PIFA with a coupling feed for quad-band operation in the mobile phone, Microwave Opt Technol Lett 50 (2008), 683–687.
20. C.H. Chang and K.L. Wong, Internal coupled-fed shorted monopole antenna for GSM850/900/1800/1900/UMTS operation in the laptop computer, IEEE Trans Antennas Propag 56 (2008), 3600–3604.
21. Y.L. Kuo and K.L. Wong, Printed double-T monopole antenna for 2.4/5.2 GHz dual-band WLAN operations, IEEE Trans Antennas Propag 51 (2003), 2187–2192.
22. Ansoft Corporation HFSS. Available at: http://www.ansoft.com/products/hf/hfss/.
23. C.T. Lee, K.L. Wong, and Y.C. Lin, Wideband monopole antenna for DTV/GSM operation in the mobile phone, Microwave Opt Technol Lett 50 (2008), 801–806.
24. SEMCAD, Schmid & Partner Engineering AG (SPEAG). Available at: http://www.semcad.com.

A MINIATURE 5.2-GHz BANDSTOP MICROSTRIP FILTER USING MULTILAYER-TECHNIQUE AND COUPLED OCTAGONAL DEFECTED GROUND STRUCTURE

Ahmed Boutejdar and Abbas Omar
Microwave and Communication Engineering, University of Magdeburg, Magdeburg, Germany; Corresponding author: ahmed.boutejdar@ovgu.de

Received 12 March 2009

ABSTRACT: *In this article, we propose a new compact defected ground structure (DGS) bandstop filter with broad pass-band, low insertion loss in the stop-band, and sharp transition from pass- to stop-band. The bandstop filter structure is simple as it is composed of a pair of octagonal DGS slots and open stubs as a compensated microstrip capacitance. The filter is realized as a multiplayer structure with wide lossless stop-band. The behavior of the filter has been investigated using EM as well as lumped-element equivalent circuit model simulations. The design equations are derived using an equivalent circuit model of a parallel* L–C *resonator. The proposed filter has been optimized, fabricated, and measured. The agreement between the simulated and measured results confirms the effectiveness of the proposed concept.*
© 2009 Wiley Periodicals, Inc. Microwave Opt Technol Lett 51: 2810–2813, 2009; Published online in Wiley InterScience (www.interscience.wiley.com). DOI 10.1002/mop.24770

Key words: *compensated-capacitor; octagonal resonator; bandstop filter; defected ground structure; reject band*

1. INTRODUCTION

Wave propagation in periodic structures has been studied in the area of applied physics for a long time [1]. Recently, periodic